Neurons from human mesenchymal stem cells display both spontaneous and stimuli responsive activity

Nihal Karakaş[1,2,*], Sadık Bay[2,¶], Nezaket Türkel[3,¶], Merve Öncül[2], Hülya Bilgen[4], Khalid Shah[5], Fikrettin Şahin[3], Gürkan Öztürk[2,6].

[1]Istanbul Medipol University, School of Medicine, Department of Medical Biology, Istanbul, 34810, Turkey

[2]Istanbul Medipol University, Regenerative and Restorative Medicine Research Center (REMER), Istanbul, 34810 Turkey

[3]Yeditepe University, Faculty of Engineering, Genetics and Bioengineering Department, Istanbul, 34755, Turkey

[4]Istanbul Medipol University Hospital, Center for Bone Marrow Transplantation, Istanbul, 34214, Turkey

[5]Center for Stem Cell Therapeutics and Imaging, Brigham and Woman's Hospital, Harvard Medical School, Boston, MA 02115, USA

[6]Istanbul Medipol University, International School of Medicine, Physiology Department, Istanbul, 34810, Turkey

¶ equally contributed

Corresponding Author:
Nihal Karakaş, M.S., Ph.D.
nkarakas@medipol.edu.tr

ABSTRACT

Mesenchymal stem cells are one of the promising tissue specific stem cell source for neural tissue regeneration applications. Previous studies on human mesenchymal stem cell (hMSC) derived neurons have been limited and not statisfactory in terms of neuronal activity. In this study, we analysed the functionality of bone marrow hMSCs differentiated into neural protein expressing cells by a single step cytokine based induction protocol. Neurons from both primary hMSCs and hMSC cell line displayed spontaneous activity (≥75%) as demonstrated by Ca^{++} imaging. Furthermore, when electrically stimulated, hMSC induced neurons (hMd-Neuron) matched the response of a typical neuron in the process of maturation. Our results reveal that enriched neurothrophic factors enhance differentiation capacity of bone marrow hMSCs into high yielding functional neurons with spontaneous activity and mature into electrophysiologically active state. hMd-Neurons have the potential to be used as a tool for disease modelling of neuropathologies and neural differentiation studies.

Key words: Mesenchymal stem cells, Neuronal differentiation, Functional neurons, Calcium imaging, Spontaneous activity, Electrophysiology

INTRODUCTION

Mesenchymal stem cells (MSCs) are heterogeneous population of multipotent and committed progenitor cells that are typically characterized by their ability to differentiate along a well-defined lineage including osteoblasts, chondrocytes, adipocytes, muscle cells, pericytes, reticular fibroblasts, and even neural cells [1-4]. A major source of these cells is the bone marrow and previous studies have shown the presence of MSCs in tissues other than the bone marrow such as dental pulp and adipose tissue as well. [5,6]. Bone marrow derived human mesenchymal stem cells (BM-hMSCs) represent an appealing source of adult stem cells for cell therapy and tissue engineering, as they are easily obtained and expanded *in vitro* while maintaining their multilineage differentiation potential [7,8]. BM-MSCs can be expanded *in vitro* without any apparent modification in phenotype or loss of function [9]. The potential use of MSCs has been reported in clinical trials that are focused on treating several diseases such as myocardial infarction, stroke, Crohn's disease, and diabetes [10].

MSCs can also differentiate into non-mesodermal lineage such as neural cells mediated by various inducers such as cytokines, cerebrospinal fluid and micro RNAs (miRNA) [1,11-13]. Previous studies have shown the neuronal differentiation capability of rat, mouse and human derived MSCs with combination of chemicals or growth factors [13]. Cytokines, growth factors, neurotrophins and retionic acid can be used to promote and support neuronal differentiation [14]. For example, when mouse marrow stromal cells were treated with epidermal growth factor (EGF) and brain derived neurotrophic factor (BDNF), neuronal markers such as NeuN and MAP-2 were detected [13].

Potent chemical reagents used for neural induction are 3-Isobutyl-1- Methylxanthine (IBMX), dibutyryl cyclic adenosine monophosphate (dbcAMP) and dimethylsulfoxide

(DMSO) [9,15]. These reagents without any growth factor addition provide only rapid neuron-like morphology acquisition [1]. Other neural induction candidates, neurotrophic factors, are essential polypeptide hormones for the development and the maintenance of the central nervous system. Neurotrophins (brain derived neurotrophic factor; BDNF, nerve growth factor; NGF and neurotrophin 3; NT-3, neurotrophin 4/5; NT-4/5), have the potential to contribute to the processes of neural fate in the stages through neurogenesis and neuroprotection. BDNF plays role in the development and maintenance of neuronal populations while NGF is also required for the development and survival of neurons [16,17]. BDNF is also involved in neurite outgrowth by binding TrkB receptor and regulates axonal and dendritic morphology [18]. Neuronal phenotype is enhanced when cytokines are enriched in neural induction media [19]. One of the major limitations in neural induction methods is the complications about neuronal phenotype, cytotoxicity of induction cocktail and insufficient functional ability of neurons [20]. Only few studies have shown that hMSC-derived neurons are functionally active upon chemical or electrical excitation [21]. Because of the complexity of the nervous system, prior to use hMSC derived neurons as a tool for disease modeling or regenerative applications, the activity pattern and functional synapse formations of these neurons have to be defined to move the neuronal differentiation study a step further [22-24].

In this study we demonstrated the ability of bone marrow hMSC derived neurons to generate spontaneous activity and respond to electrical stimulation. Herein, we introduce hMSC-derived neurons (hMd-Neurons) with high functional neuronal ratios in a defined induction media that can be further studied and potentially link the technical bridges to broadly study the nervous system deficiencies.

MATERIALS and METHODS

Cell lines and Reagents

Human bone marrow derived mesenchymal stem cell (hMSC) line (UE7T-13 cells, no. RBRC-RCB2161; RIKEN, Japan) [20,25-28], Growing and expansion media of hMSCs: Dulbecco's Medified Eagle's Medium (DMEM; Gibco) with 2mM L-Glutamine, Fetal bovine serum (FBS; Gibco), Penicillin/Streptoycin (Gibco). Neuronal induction: dibutyryl cyclic AMP (dbcAMP; Sigma), 3-isobutyl-1-methylxanthine (IBMX; Sigma), human epidermal growth factor (hEGF; Sigma), recombinant human basic fibroblast growth factor (bFGF; R&D systems), fibroblast growth factor-8 (FGF-8; Pepro Tech), recombinant human brain-derived neurotrophic factor (BDNF; R&D systems), and nerve growth factor (NGF), Neurobasal medium (Gibco) supplemented with 2% B27 supplement (Gibco), 2 mM L-glutamine (Gibco).

Sample collection and ethical issues

Human bone marrow aspirates of healthy donors were supplied by Istanbul Medipol University, Center for Bone Marrow Transplantation. Bone marrow samples (n=5, 1 female and 4 males) were collected from healthy donors from ages 2-18 and used in this study. Written consents of donors (parents of the matched allogeneic donors) were obtained, documented and witnessed. While doing the harvesting of the bone marrow for transplantation, 20 ml/ kg of donor bone marrow was harvested (400-1000 ml) and 5 ml was kept for the study. The 395-995 ml was infused to the patient. All procedures were approved by Ethics Committee of Author University. (no.425 on 10.25.2017)

Isolation and Expansion of Bone Marrow Mesenchymal Stem Cells

Human mesenchymal stem cells (hMSCs) were isolated from bone marrow by ficoll density gradient centrifugation. After isolation, cells were cultured in Dulbecco's Modified Eagle Medium-low glucose (DMEM-LG, Gibco) culture medium containing

20% fetal bovine serum (FBS, Gibco) and 0.2 % primocin (Gibco). Cells were incubated at 37°C in a humidified 5% CO_2 chamber. Then, non-adherent cells were removed via medium refreshment after 3 days (d) and adherent cells were labeled as passage 0 (P0) and grown to 80% confluence. When the cells reached 80% confluence, they were detached with 0,25 % Trypsin/EDTA solution. The cells were harvested and subcultured at a density of 1.5 x10^3 cells/cm^2 in culture flasks per 5-6 days. Flow cytometry analysis was performed at passage 3 (P3) and each donor derived hMSCs were processed in the same order and used for all experiments.

Flow Cytometry

To confirm hMSC phenotype of isolated cells grown in culture, cells were subjected to flow cytometry analysis. Flow cytometry was performed using a FACS (BD Influx Cell Sorter with Bioprotect IV Safety Cabinet) system. The data were analysed with FlowJo software (Treestar) and the forward and side scatter profile gated out debris and dead cells. Immunophenotyping of human BM-MSCs was performed with antibodies against the following human antigens: CD14 (Abcam-ab82434), CD29 (Biolegend-303004), CD31 (Abcam-ab27333), CD34 (Abcam-ab18227), CD44 (Abcam-ab58754), CD45 (Abcam-ab134202), CD73 (Abcam-ab157335), CD105 (Abcam-ab53321), and their isotype controls. For determining whether proliferating neural stem/progenitor cells are present among hMd-Neuron, we analysed cell fractions of hMd-Neurons by Nestin (BD-51-9007230), Ki-67 (BD-51-9007231) and Sox-2 (BD-51-9007227) antibodies.

Mesodermal Differentiation

To qualify isolated cells from BM as MSCs, cells were induced for differentiation into adipogenic, osteogenic and chondrogenic lineages. Briefly, for adipogenic differentiation, 5x10^3 hMSCs/cm^2 were exposed to Complete MesenCult Adipogenic Medium containing MesenCult MSC Basal Medium (Stemcell) and 10% Adipogenic

Stimulatory Supplement (Stemcell) for 3 weeks. For osteogenic differentiation, $2x10^5$ cells/cm^2 incubated with Complete MesenCult Osteogenic Medium including MesenCult MSC Basal Medium, Osteogenic Stimulatory Supplement, β-Glycerophosphate, Dexamethasone, Ascorbic acid (all from Stemcell) for 5 weeks. For chondrogenic differentiation, $7.5x10^6$ cells/cm^2 were cultured for 3 weeks with Stempro Chondrocyte Differentiation Basal Medium (Gibco) containing 10% Stempro Chondrogenesis Supplement (Gibco). Standard histochemical staining methods were applied. Osteogenic, adipogenic and chondrogenic differentiation were confirmed by Toluidine Blue, Oil Red O, Alcian Blue staining, respectively.

Neuronal Induction

For neural induction experiments, we used a commercial hMSC cell line (UE7T-13 cells, no. RBRC-RCB2161; RIKEN, Japan) and hMSCs isolated from 5 different healthy donors. We repeated experiments for each hMSC donors used in this study. hMSCs at P3 were seeded on culture dishes prior to neuronal induction. Cell density was optimized to $3,0x10^3$. Culture was maintained via using DMEM containing 10% FBS and cells were incubated in 37°C, 5% CO_2 incubator for 24 hrs. Neuronal induction media was prepared with 20 ng/ml hEGF, 40 ng/ml bFGF, 10 ng/ml FGF-8, 10 ng/ml human BDNF, 40 ng/ml NGF, 0.125 mM dbcAMP, 0.5 mM IBMX, 2 mM L-glutamine in Neurobasal medium + B27 supplement in the absence of serum. Cells were then treated with neuronal induction media by medium refreshment every 48 hours throughout the differentiation process. In line with this, samples were collected for reverse transcriptase PCR (RT-PCR) at distinct time points (d0, d2, d6, and d12).

Time Dependent Cell Response Profiling (RT-CA)

We used a real time cell analysis system, xCELLigence RT-CA (Roche) to monitor motility of hMSCs. The system detects impedence changes within multiwells that contain electrode arrays at the bottom (E-plates). As the culture cells multiply, this

increases impedence and an upward deflection is recorded in the *cell index*. Therefore, proliferating and migrating hMSCs show an increasing cell index, while neuronal differentiated hMSCs are expected to display stable cell index related to their decreased motility. Before starting the experiments background readings were made by culture medium only. Then, $3x10^3$ hMSCs were added to each well in expansion medium, which was replaced with the neuronal induction medium 24 hours later. The induction medium was replaced every 48 hours. The E-Plates containing the cells were placed on the reader in 37°C, 5% CO_2 incubator for cell index recording for 12 days.

Cell Viability Assays

For analysis of cell death on neuronal induced hMSCs, cells were seeded on 96 well plates for Annexin-V and Sytox green stainings. Cells were treated with NI media and apoptosis was induced in positive control cells by treatment with camptothecin (Sigma). The medium was removed from the wells, cells were fixed with 4%PFA and 100 µl of Annexin-V-Alexa 568 labeling solution (Roche) and 50 µM Sytox Green dye (Invitrogen) was added to each well. After 10 or 15 minutes incubation at 15 to 25°C, wells were washed with PBS. As for nuclear staining, cells were treated with 1:15000 DAPI (Sigma) for 10 minutes at RT. Wells were washed with PBS and dH_2O subsequently. The cells were analyzed by fluorescence microscopy (Zeiss Inverted Microscope with Hoffman Modulation).

Reverse Transcriptase PCR (RT-PCR)

RNA samples of hMSC were extracted by using RNeasy kit (Qiagen). 0.5 µg of total RNA was reverse transcribed to obtain cDNA by Quantitect Reverse Transcription kit (Qiagen). cDNA library was obtained after 35 cycles of amplification (PCR core kit, Qiagen). Primer pairs (Forward; Fw and reverse; Rv) used in the experiments as follows: βIII tubulin (Fw: 5'-AGTGATGAGCATGGCATCGA-3' and Rv: 5'-

AGGCAGTCGCAGTTTTCACA-3' generating a 317 bp fragment; NSE (Fw: 5'-CCCACTGATCCTTCCCGATACAT-3' and Rv: 5'-CCGATCTGGTTGACCTTGAGCA-3' generating a 254 bp fragment; NF-L (Fw: 5'-TCCTACTACACCAGCCATGT-3' and Rv: 5'-TCCCCAGCACCTTCAACTTT-3' generating a 1113 bp fragment; Nestin (Fw: 5'-TGGCTCAGAGGAAGAGTCTGA-3' and Rv: 5'-TCCCCCATTTACATGCTGTGA-3' generating a 148 bp fragment. A human GAPDH primer pair (Fw: 5′-GTCAGTGGTGGACCTGACCT-3′, Rv: 5′-TGCTGTAGCCAAATTCGTTG-3′) generating a 245 bp fragment was used as a positive control.

Immunofluorescent Staining

hMd-Neurons were analysed for neuron spesific phenotypical characteristics at day 12 of neuronal induction. Each staining was performed as triplicated wells and repeated for each donor. Cells were fixed with 4% paraformaldehyde in phosphate buffer saline (PBS, Sigma) and incubated at RT for 15 minutes. After washing with PBS, cells were blocked with the solution containing 1% Goat serum (Sigma), 3% BSA (Sigma), 0.3% Sodium azide (Sigma), and 0.1% Triton X-100 in PBS. After discarding blocking solution, cells were treated with primary antibodies against neuron specific enolase (NSE (2.5 µg/ml diluted), Abcam-ab53025), neuronal specific nuclear protein (NeuN (1:500 diluted), Abcam-ab104224), protein gene product 9.5 (PGP9.5 (1:100 diluted), Abcam-ab8189), microtubule associated protein 2 (Map2 (1:500 diluted), Sigma-M1406), neurofilament 200 (NF200 (1:200 diluted), Abcam-ab4680), Synaptophysin ((1:500 diluted) Abcam-17785-1-AP) and PSD-95 ((2.5 µg/ml diluted) Abcam-ab12093) using desired concentrations in PBS containing 3% BSA (Sigma), 0.3% Sodium azide (Sigma), %1 Tween20 and 1% Goat serum (Sigma) at 4^{o}C for o/n. After antibody treatment, wells were washed with PBS and incubated at room temperature for three hour with 1:200 diluted goat anti-mouse (GAM) IgG Alexa Fluor 488 (ab150113), 1:200 diluted goat anti-rabbit (GAR) IgG

Alexa Fluor 488 (ab150077), 1:200 diluted donkey anti-goat (DAG) IgG Alexa Fluor 568 (ab175474), 1:500 diluted goat anti-rabbit (GAR) IgG Alexa Fluor 594 (ab150088) and 1:100 diluted goat anti-chicken (GAC) IgG Alexa Fluor 633 (A-21103) secondary antibodies. After washing with PBS, cells were treated with 1:15000 DAPI solution and incubated at RT for 3 minutes. Wells were washed with PBS containing 0.1% sodium azide and slides were mounted with vectashield mounting medium (Vectorlab). Cell images were taken with fluorescent microscope (Zeiss LSM780 Confocal Microscope).

Calcium imaging

To analyse changes in Ca^{++} concentration in neurons from human bone marrow mesenchymal stem cells (hMd-Neurons), we used Fluo-4 staining (ThermoFisher) between day5-day18 of neuronal induction. Briefly, medium was aspirated and washed with Hank's Balanced Salt Solution (HBSS, Sigma) and Tyrode's solution. Cells were treated with staining solution containing Fluo-4, pluronic acid and Tyrode's solution at room temperature for 30 minutes. After discarding staining solution, cells were washed with Tyrode's solution and HBSS. Cells were incubated at 37^{o}C for 10 minutes in induction medium. Then, fast imaging was done on Zeiss Cell Observer SD Spinning Disk Time-Lapse Microscope. Calcium imaging was performed for 150-250 cells for each group and repeated for different donors as well.

Electrophysiology

We maintained hMd-Neuron culture for longer periods of time in NI media to enable progress in neuronal maturation. Before patch clamp recordings to determine the viability of neuronal induced hMSC for longer culture periods (during 21 days), we used CellTiter Glo Viability Assay (Promega) following the protocol according to manufacturer's instructions. A 15 mm coverslip containing donor derived hMd-Neurons at day 5-18 of neural induction was placed into the recording chamber.

Cultured cells were perfused with aCSF (artificial cerebrospinal fluid) containing the following (in mM): 150 NaCl, 10 D-glucose, 4 KCl, 2 $MgCl_2$, 2 $CaCl_2$, and 10 HEPES, aerated with 95% O_2, 5% CO_2 delivered at a rate of 2-3 ml/min. The cells were identified and targeted using an Olympus microscope and were patched using pipettes with 3-6 MΩ tip resistances in the bath when filled with an internal solution. Whole cell voltage-clamp recordings were performed using pipettes (Harvard Apparatus) made from borosilicate glass capillaries pulled on a Flaming-Brown micropipette puller (Model P-1000, Sutter Instruments, Novato, CA). Pipette solution contained (in mM): 125 CsCl, 5 NaCl, 10 HEPES, 0.6 EGTA, 4 Mg-ATP, 0.3 Na_2GTP, 10 lidocaine N-ethyl bromide (QX-314), pH 7.35 and 290 mOsm. The holding potential was set to -60 mV. Electrical stimulation performed using a field electrode that was placed within adjacent to the coverslip. Half-maximal stimulus strength was used for electrical stimulation, we waited at least 200 milliseconds between successive field stimuli. All experiments were performed at room temperature as triplicates.

Statistics

Statistical comparisons were performed by *t*-test and/or two-tailed *t*-test assuming equal variance. Differences were considered as statistically significant at $p^{***} < 0.0001$. Data are the mean ± standard error (SE). One-way analysis of variance (ANOVA) was used to evaluate the differences in cell death levels among three groups. An alpha value of $p^{\#} < 0.05$ was used for statistical significance.

RESULTS

Functional neurons *(hMd-Neurons)* can be yielded with high ratios from hMSCs *in vitro*

To study neuronal differentiation of hMSCs, we initially used human bone marrow hMSC cell line (UE7T-13 cells, no. RBRC-RCB2161; RIKEN, Japan) [20,25-28]. To improve *in vitro* generation of neuronal cells with sufficient differentiation capacity, we used a non-viral neuronal induction method which is an enriched form of previously defined combination [19]. Neuronal cell morphology was observed within 24hrs upon neuronal induction (NI) and almost all hMSC cell line gave rise to bipolar neuron-like cells with neuritis (Fig. 1A).

Figure 1. Human bone marrow MSC cell line have the ability to differentiate into spontaneously active neurons (A) Schematic representation of neuronal induction on hMSC cell line. (B) Plot indicates neuronal markers expression percentages of hMd-Neurons from hMSC cell line after neuronal induction during 12 days and almost %100 of neuronal induced cells express neuronal maturation proteins NeuN, Synaptophysin, NSE and PGP 9.5. Positively stained cells counted from 10 different area of staining and averages were calculated. Functionality of hMd-Neurons was evaluated upon labeling with Fluo-4 for real time Ca^{++} ion imaging without any outside stimulation chemically. (C) Immunofluorescence co-staining of hMSC cell lines in neuronal induction medium; NIM composed of NGF, BDNF, FGF-8, bFGF, EGF, dbcAMP, IBMX, B27 for 12 days reveals the presence of neuronal maturation proteins NeuN (a, e) and Synaptophysin (b, f) with DAPI nuclear staining (c, g). Merged images represent positive co-staining of NeuN and Synaptophysin for each individual cell (d, h). Dashed yellow squares magnified 3 folds (d', h'). (D) Florescent images (a-f) demonstrates time dependent firing pattern of hMd-Neurons from hMSC cell line through imaging of Ca^{++} ion kinetics and arrows indicate firing of each hMd-Neuron separately (sec; seconds). (Video 1) (E) Histogram indicates firing frequency and signal intensity of each individual hMd-Neurons while there is no signs of spontaneous activity from uninduced hMSCs. According to Ca^{++} influx/efflux through

hMd-Neurons, (F) 78.5 % of cells were recorded as spontaneously active with twice firing frequency in 4 minutes. Data are represented as mean ± S.E.M. Scale bars represent 50μm.

For neuron specific characteristics, we stained hMd-Neurons for neuronal markers including NF, NeuN, NSE, PGP 9.5, as well as synaptic proteins Synaptophysin, and PSD 95 on day 10 of NI. hMd-Neurons showed expressions of all neuronal markers with high percentages (Fig. 1B-C, and Figure S1). To evaluate spontaneous activity of hMd-Neurons, we performed live cell Ca^{++} imaging without any chemical addition, which showed Ca^{++} transients in differentiated hMSCs. More than 78% of hMd-Neurons were spontaneously active neurons showing Ca^{++} concentration changes without any stimulation. They showed spontaneous activity that is not induced by an external stimulus with different firing patterns [29] (Fig. 1D-F, and Video 1).

Figure S1. Neuronal marker expressions of hMd-Neurons from hMSC cell lines

(A) hMSC cell line was stained for distinct neuronal protein expressions and almost %100 of neuronal induced hMSCs were identically positive for PGP 9.5 (a) and NSE (d) with DAPI nuclear stain. Merged images of PGP 9.5 and NSE (c, f) magnified 4 folds respectively (c', f'). Scale bars represent 50 μm.

Isolated cells from healthy bone marrow donors represent hMSC phenotype

After yielding functional neurons from hMSC cell line, we then studied neuronal differentiation of hMSCs from healthy human bone marrow donors in detail. We first showed that cells isolated from human bone marrow are MSCs in agreement with the criteria of International Society for Cellular Therapy published in 2006 [7]. During initial phases of culture, non-adherent cells were depleted and very small proportion of the cells attached on plastic culture surface. These cells had a fibroblast-like

morphology, formed colonies and by passage 3 (P3), more than 95% of the cells were MSCs as revealed by flow cytometry analyses. Results from different healthy donors indicated that these adherent cells at P3 have hMSC immunophenotype with negative expression of CD45, CD34, CD14 and CD31 while they were positive for CD29, CD44, CD73, and CD105 (Fig. 2A, B).

Figure 2. Isolated cells from bone marrow stroma of healthy donors display typical hMSC phenotype and mesodermal differentiation capacity (A, B) After isolation of human bone marrow cells from healthy donors, cells at passage 3 were analyzed by flow cytometry for phenotypic characterization. The cells showed hMSC specific marker expressions with negative expression of CD14, CD31, CD34, and CD45, while they were positive for CD29, CD44, CD73 and CD105. Representative histograms and surface antigen profiles of isolated adherent cells from 5 healthy donors are demonstrated. (C) Adipogenic differentiation was confirmed by Oil Red-O staining of lipid vacuoles (with hematoxylin counterstain); osteogenic differentiation was followed with Toluidine Blue staining of Calcium deposits showing mineralization; and Alcian Blue staining of proteoglycans in chondrogenic pellet demonstrated chondrogenic differentiation.

For lineage specific MSC differentiation ability, we analysed mesodermal differentiation (adipogenic, osteogenic and chondrogenic) of immunophenotyped hMSCs. To demonstrate adipogenic differentiation of hMSCs, we used Oil Red-O, which labels neutral triglycerides, lipids and lipoproteins. For detection of chondrogenic differentiation, Toluidine Blue-O and Alcian Blue stains were applied; while the former stains calcium deposits indicative of mineralization, the latter turns chondrogenic spheroids into dark blue which marks the extracellular matrix of cartilage (Fig. 2C). Positive stainings were counted for each from 10 different

independent fields and the differentiation percentages were then determined. Depending on 50% chondrogenic, 43% osteogenic and 52% adipogenic differentiation rates, we concluded that more than 95% of the cells from bone marrow were hMSCs at P3 in our experimental paradigm.

Donor derived hMSCs can also differentiate into *hMd-Neurons*

We maintained NI for 12 days prior to phenotypical/functional characterization of neuronal induced hMSCs from bone marrow donors and their neuronal morphology in culture was variable (Fig. 3A). Morphologically neural like cells with neurite extensions were counted from 10 different independent fields and the neural morphology percentages were then determined. On one hand, hMSCs derived from bone marrow donors showed neural morphology (65%) at day 1 of NI while neuronal cell percentage was increased to 80% by day 3 (Figure 3S-a, b). We determined the highest proportion of neural cells from hMSC donors as 85% at day 5 (Figure S3), which slightly increased up to 90-95% at day 12 (Fig. 3B).

Figure 3. Bone marrow hMSCs from healthy donors differentiated into hMd-Neurons with phenotypical characteristics (A) Schematic representation of neuronal induction on bone marrow derived hMSCs from healthy donors. (B) Bright field images represents almost %90 of neuronal induced human bone marrow donor derived hMSCs give rise morphologically variable neuron like cells on culture at day 12 (b, d) whilst uninduced hMSCs maintains proliferation (a, d). Morphology of hMd-Neuron from human samples varies in culture as seen with neurite extension patterns (b, d). (Figure S3). (C) Representative florescent images of Annexin V/Sytox green stainings showing cell viability of neuronal induced hMSCs with positive control stainings of dead cells on camptothecin (CAM) treated uninduced hMSCs. (D) Positively stained cells from Annexin V and sytox green stainings of 3 different

donors were counted and the percentages of dead cells were determined. Plots indicate dead cell percentages from d2 to d12 in CAM treated, untreated (in growth medium), and neuronal induced hMSCs. (E) Graph showing time dependent cell proliferation profile of uninduced and neuronal induced hMSC during 12 days in culture by X-Celligence (Roche) real time cell analysis (RT-CA) system (F) RT-PCR demonstrating presence of βIII tubulin, Nestin, NSE, NF transcripts during neuronal differentiation (d2-d12) respectively versus an absence in uninduced hMSCs (d0). (G) Plots indicating neuronal marker expression percentages ≥%89 (Images from 3 different donors were counted to determine the neuronal marker percentages). Positively immunostained cells counted from 10 different areas of stainings and averages were calculated. (H) Representative confocal images showing neuronal protein expressions; NSE, PGP 9.5 and NeuN respectively (a, d, g) with DAPI nuclear stainings (b, e, h) of hMd-Neurons at d12 after neuronal induction. Fluorescent images of neuronal protein expressions merged with DAPI staining (c, f, i). (I) Plots represents flow cytometry results indicating 99.24% of hMd-Neurons are Nestin positive and negative for Ki-67 proliferation marker and Sox-2 expressions at day6of NI. (J) Flow cytometry analysis indicates loss of Ki-67 proliferation marker and Sox-2 expressions in Nestin positive cells. Scale bars represent 100 μm. Data are represented as mean ± S.E.M. Significance of ANOVA test *** p <0.0001.

Figure S3. Neuronal cell morphology with neurite extensions appears by day 1 of hMSC neuronal induction (A) Bright field images represent morphology of hMd-Neurons from healthy bone marrow donors in culture by d1, d3 and d5 (a, b, c) . Images were taken under 10X. Dashed squares magnified 2 folds respectively (a', b', c'). Arrows indicate neurite to neurite and neurite to cell body end points.

Prior to further analysis on hMd-Neurons from bone marrow donors, we determined the toxicity of neuronal induction media (NI). For this, we evaluated cell death and apoptosis during neuronal induction of hMSCs from bone marrow donors at day2, day6, and day12. An apoptosis inducer camptotechin (CAM) was used as a positive control. Annexin-V and Sytox Green stainings showed that while 89±11% of CAM-treated cells were dead at day 2, neuronal induced hMSC were viable with a high rate comparable to uninduced control cells. At day 6, we observed 90±6%, 10±3%, and 4.5±2% of dead cells in CAM-treated, uninduced and neuronal induced cells, respectively. At day 12, 94±4%, 20±3% and 10±2% of cells were dead in CAM treated, uninduced, and neuronal induced cells, respectively. Of all dead cells 99±2%, 99±2% and 99.5±1% of hMSCs were apoptotic in CAM group at day 2, 6 and 12, respectively. In the uninduced group 1±0.8% and 15±2% apoptotic cells were observed only at day 6 and day 12. In contrast, a no significant number of apoptotic cells were observed in NI group at any time point (Fig. 3C, D). Next, we investigated cell kinetics of differentiated versus undifferentiated hMSCs by real time cell analysis depending on cel motility changes (named as cell index) (XCelligence, Roche). The recordings suggest that the number of uninduced hMSCs incresad steadily while hMd-Neurons showed a stable cell index by day2 of NI. In addition to that, cell index was stabilized around day 6 of NI at which cells might commit to attain neuronal characteristics (Fig. 3E).

As a phenotypical outcome of neuronal differentiation, we assessed neuronal transcripts of βIII Tubulin, Nestin, NSE, NF, and a housekeeping gene (*GAPDH*). RT-PCR results indicated that donor derived hMd-Neurons have transcripts of early neuronal marker NSE by day 2 and late neuronal marker NF by day10. Transcripts of βIII Tubulin and Nestin were detected during all stages of differentiation. However, uninduced hMSC also had βIII Tubulin and Nestin mRNAs (Fig. 3F), which has also

been previously reported [15-17,30]. Next, we showed neuronal protein expressions on donor-derived hMd-Neurons on day 12 of neuronal induction (NI) by immunofluorescence staining. More than 90% of hMd-Neurons showed expressions of neuronal markers NF, NeuN, NSE, PGP 9.5, as well as synaptic proteins Synaptophysin, and PSD 95 (Fig. 3G, H).

hMSCs preserve *Nestin* whereas they loose *Ki-67* and *Sox-2* expression during differentiation into *hMd-Neurons*

To examine the differentiation process of hMd-Neurons, we evaluated the fractions of Nestin and Sox-2 positive cells in hMd-Neurons at day 6. We also included Ki-67 as a marker for proliferating cells. Flow cytometry analysis (single channel) showed that among hMd-Neurons from healthy donors 99% were Nestin positive; 96% of cells were Ki-67 and Sox-2 negative (Fig. 3I). Accordingly, multichannel records revealed that almost 90% of Nestin positive cells were Sox-2 and Ki-67 negative whilst Nestin positive (Fig. 3J). This data correlated with the presence of Nestin transcripts during neuronal differentiation (Fig. 3F). Assembly of data from mature protein expressions and lack of neural stem cell and proliferation markers suggests that phenotype of hMd-Neurons by day 6 is a neuronal cell type rather than a neural stem/progenitor cell type.

***hMd-Neurons* from healthy bone marrow donors mature into both electrophysiologically and spontaneously active neurons**

To study functionality of hMd-Neurons from health bone marrow donors, we stained their *in vitro* neuronal connections for presynaptic (Synaptophysin) and postsynaptic (PSD95) proteins and they were positive for both synaptic markers (Fig. 4A).

Figure 4. Donor derived hMd-Neurons mature into functional neurons with both spontaneous and electrophysiological activity Confocal images of neuronal induced hMSCs from healthy bone marrow donors (2-10 aged) at day 12 reveals the expression of synaptic proteins (a) Synaptophysin and (b) PSD-95 with (c) DAPI nuclear stainings. Merged image represents positive co-staining of Synaptophysin and PSD-95 for each individual hMd-Neurons (d). Dashed yellow squares magnified 5 folds (d'). Functionality of hMd-Neurons was evaluated using Fluo-4 Calcium indicator for real time Ca^{++} ion imaging without any stimulatory chemical addition. (B) Florescent images (e-i) represents real time firing patterns of hMd-Neurons from hMSCs via imaging of Ca^{++} signal transmission through a single neuron and arrows indicate initiation and termination of firing in seconds (sec). (Figure S4 and Video 2). (C) Representative histogram indicates firing frequency of each individual hMd-Neurons as twice in less than 1 minute. No signs of activity of uninduced hMSCs of the same donors were detected. (D) Upon imaging Ca^{++} ion dynamics, 74,6 % of cells were counted as spontaneously active according to firing situation (percentages were determined from average of 3 different donors). (E) Represantative patch clamp (whole cell) recordings of 18 days neuronal induced hMSC from donors. (F) Prior to electrophysiology experiments, long term hMd-Neurons viability was evaluated for further maturation in culture using Cell Titer Glo (Promega) assay. Data are represented as mean ± S.E.M. Scale bars represent 50 μm.

Figure S4. Real time firing pattern of hMd-Neurons from donor derived hMSCs in a group of cells within 90 seconds (A) Florescent images (a-e) demonstrates time dependent firing pattern of hMd-Neurons from donor derived bone hMSC through imaging of Ca^{++} ion influx/efflux. Numbers indicate firstly tracked signal input (1-3) and output (1' and 2') in images for some of the hMd-Neurons separately. Images were taken under 20X.

We then evaluated their Ca ion flux as we demonstrated for hMSC cell line derived hMd-Neurons. We recorded spontaneous activity of donor-derived hMd-Neurons through Ca ion imaging (Fig. 4B, Figure S4 and Video 2 and Video 3). No activity was detected from uninduced hMSCs (Video 4). Donor derived hMd-Neurons showed individual differences in terms of firing frequencies (average was twice in less than 1 minute) (Fig. 4C). Among all hMd-Neurons, around %75 were spontaneously active neurons (Fig. 4D).

In addition to Ca^{++} imaging, we evaluated neuronal functionality by patch clamp technique. Prior to experiments we cultured hMd-Neurons for 18 days to let maturation of their electrical properties. We also recorded directly from donor-derived hMd-Neurons to characterize their electrophysiological properties. We applied electrical stimulation to activate the cells and then hMd-Neurons generated action potentials upon electrical stimulation in miliseconds similar to a maturating neuron (Fig. 4E). We also showed that hMd-Neurons could survive as monolayers over long periods in NI media without the addition of any extracellular matrix proteins or coating materials (Fig. 4F).

DISCUSSION

One of the main concerns about studies with neuronal differentiation of hMSCs is establishing a succesful induction method leading to sustainable and high yields of functional neurons [31]. In this study, we showed that bone marrow hMSCs either from cell line or healthy donors differentiate into functional neurons (>74%) by a single step protocol. hMSC derived neurons (hMd-Neurons) displayed spontaneous activity and showed response in miliseconds to electrical stimulation as a typical maturating neuron [32].

We first focused on the phenotype of neuronal induced hMSC cell line and donor derived hMSCs prior to functionality analysis. Immunostainings showed that induced hMSCs in the presence of EGF, bFGF, NGF, BDNF, FGF-8, dbcAMP and IBMX are able to progress into neuronal differentiation with positive expressions of neuron specific proteins (Nestin, NeuN, NF, Synaptophysin, PSD95, PGP9.5). Moreover, we detected Nestin expression during 12 days of neuronal differentiation whereas proliferating cells had depleted Nestin expressions. Accordingly, our cell fractionation analysis for neuronal induced hMSCs showed that almost 90% of Nestin positive cells were also negative for Ki-67 and Sox-2 indicating that they were in the process of neuronal maturation. Additionally, real time cell response of neuronal induced hMSCs also supported that on the way to differention into hMd-Neurons, proliferation modalities were downregulated which associates with post-mitotic nature of mature neurons. Existance of neuronal phenotype of hMd-Neurons was also seen in neurite outgrowths which is also crucial for the establishment and maintanance of neuronal networks [33]. hMd-Neurons exhibit neurite to neurite and neurite to cell body end points which evokes axoaxonic/axodentric and axosomatic synapses. First set of experiments remarkably revealed the dominant neuronal characteristics of induced hMSCs from both cell line and bone marrow donors, then ultimately we focused on inquiries about neuronal functionality and activity ratio of hMd-Neurons.

Functional connections on hMd-Neurons were initially profiled for the expression of presynaptic (Synaptophysin) and post-synaptic (PSD95) proteins as synaptic formation is required for communication of neurons in their own network. hMd-Neurons from both hMSC cell line and primary hMSCs visibly built synaptic connections *in vitro*. We then monitored Calcium ion exchange to determine activity of hMd-Neurons. Surprisingly, we could detect spontaneous activity of hMd-Neurons both from hMSC cell line and donor derived hMSCs without any stimulatory chemical

addition [34-36]. This is a phenomenon that can be discussed since spontaneous activity is not an ability of all primary neurons. For instance, when Calcium ion imaging applied, mouse derived dorsal root ganglia (DRG) neurons are quiescent (no activity) while cortical neurons display firing pattern spontaneously even at high frequencies [37,38]. Therefore further investigations are required on hMd-Neurons (or other functional neurons derived from stem cells) to well (explicitly) define their abilities and tissue/function specific phenotypes.

Another outcome of Calcium imaging experiments showed that timing of Ca^{++} ion flux of hMd-Neurons was varying. Mainly, spontaneous activity of hMd-Neurons was recorded at day 5. On the other hand, hMSCs from one of the donors were able to function prior to day 5 of NI. What is more, hMSCs from one of the donors displayed spontaneous activity around day 8 while no signals were recorded at day 5. Regardless of difference in activation time point, all of the donors sustained the functionality during their *in vitro* neuronal maturation. Overall, hMd-Neurons mostly showed activity at day 5, our data pointed out individual differences of hMSC sources in terms of neuronal functionality timing.

Following the neuronal activity records, we further investigated the excitability of hMd-Neurons from 5 different human bone marrow donors to test their synaptic functionality. According to patch clamp results hMd-Neurons were electrophysiologically active and showed a similar response pattern of a neuron on maturation [39]. Additionally, improvement of the culture conditions using tissue engineering tools, which mimicks neuronal microenvironment can be applied to study maturation process of hMd-Neurons thoroughly. These studies will maximize to understand abilities of hMd-Neurons to form functional neural networks and this is an avenue that we are actively pursuing.

In terms of comparing hMd-Neurons from MSC cell line and primary hMSCs, we observed that hMd-Neurons from hMSC cell lines were identical and mostly had bipolar structures. Otherwise, hMd-Neurons from human bone marrow donors displayed heterogenity in neurite extension patterns. This explains that since cells of hMSC cell line are genetically identical, they give rise to less complex neurons with structural similarities. Conversely, primary hMSCs from bone marrow donors might have different subpopulations with seperate differentiation abilities. Therefore immunophenotyping of isolated cells from bone marrow as hMSCs only allows researchers to classify hMSCs for general characteristics and not for their differentiation capacity leading to specific type of a neuron. Furthermore, hMd-Neurons can be served as a potential candidate to highly yield certain types of neurons such as Dopaminergic, Gabaergic neurons etc. as many researchers focused on this field for therapeutic applications [40-42]. One solution to that might be investigation of hMSC subpopulations that have the potential to differentiate into a specific neuron type with high purity under certain conditions. Similar approach was previously reported to successfully yield neurons from Nestin positive hMSCs [43,44]. Adopting it to obtain function/tissue specific neurons from hMSC subtypes can be a clonogenic based approach for neural differentiation studies. We are in the process of derivation of functional hMd-Neurons according to hMSC subtype. Furthermore, categorization of hMd-Neurons according to their structural class, homing certain types of neurotransmitter receptors, and overall investigation of their function/tissue spesific abilities can pioneer the regenerative studies for a broad range of the nervous system deficiencies and ultimately lead to development of disease models and preclinical therapeutic approaches [45,46].

Taken together, our findings introduce functional hMd-Neurons, that can be easily obtained *in vitro* either from hMSC cell line or donor derived hMSCs through a

defined induction protocol. According to these outcomes, in vitro characterization of hMd-Neurons for spesific neuronal subtypes; hMd-Neuron derivation from patients with neuropathologies and their *in vivo* functional abilities can be further evaluated. Therefore, hMd-Neurons can be utilized for a wide range of applications including, disease modeling; tissue engineering approaches; studying the mechanism of neuronal differentiation; and understanding hierarchic establishment of newborn neurons from hMSCs.

AUTHOR CONTRIBUTIONS

N.K.: Conception and design, Provision of study material, Collection and assembly of data, Data analysis and interpretation, Manuscript writing, Final approval of manuscript; S.B.: Collection and assembly of data, Data analysis and interpretation, Final approval of manuscript; N.T.: Data analysis and interpretation, Manuscript writing, Final approval of manuscript; M.O.: Collection and assembly of data, Data analysis and interpretation, Final approval of manuscript; H.B.: Provision of study material, Data analysis and interpretation, Final approval of manuscript; K.S.: Data analysis and interpretation, Manuscript writing, Final approval of manuscript. F.S.: Data analysis and interpretation, Manuscript writing, Final approval of manuscript; G.O.: Data analysis and interpretation, Manuscript writing, Final approval of manuscript.

ACKNOWLEDGEMENTS

We thank to Deniz Atasoy for his contributions in patch clamp data records and analysis. We also thank to Emre Vatandaslar for flow cytometry data processing.

This work was funded by Istanbul Medipol University, Regenerative and Restorative Medicine Research Center (REMER) and Yeditepe University, Department of Genetics and Bioengineering.

CONFLICT OF INTEREST

Authors declare no conflict of interest.

REFERENCES

1. Woodbury D, Schwarz EJ, Prockop DJ, Black IB (2000) Adult rat and human bone marrow stromal cells differentiate into neurons. J Neurosci Res 61: 364-370.
2. Pittenger MF, Mackay AM, Beck SC, Jaiswal RK, Douglas R, et al. (1999) Multilineage potential of adult human mesenchymal stem cells. Science 284: 143-147.
3. Abouelfetouh A, Kondoh T, Ehara K, Kohmura E (2004) Morphological differentiation of bone marrow stromal cells into neuron-like cells after co-culture with hippocampal slice. Brain Res 1029: 114-119.
4. Cano E, Gebala V, Gerhardt H (2017) Pericytes or Mesenchymal Stem Cells: Is That the Question? Cell Stem Cell 20: 296-297.
5. Zeng G, Lai K, Li J, Zou Y, Huang H, et al. (2013) A rapid and efficient method for primary culture of human adipose-derived stem cells. Organogenesis 9: 287-295.
6. Honda MJ, Watanabe E, Mikami Y, Saito Y, Toriumi T, et al. (2013) Mesenchymal dental stem cells for tissue regeneration. Int J Oral Maxillofac Implants 28: e451-460.
7. Fakhry M, Hamade E, Badran B, Buchet R, Magne D (2013) Molecular mechanisms of mesenchymal stem cell differentiation towards osteoblasts. World J Stem Cells 5: 136-148.
8. Catacchio I, Berardi S, Reale A, De Luisi A, Racanelli V, et al. (2013) Evidence for bone marrow adult stem cell plasticity: properties, molecular mechanisms, negative aspects, and clinical applications of hematopoietic and mesenchymal stem cells transdifferentiation. Stem Cells Int 2013: 589139.
9. Lu P, Blesch A, Tuszynski MH (2004) Induction of bone marrow stromal cells to neurons: differentiation, transdifferentiation, or artifact? J Neurosci Res 77: 174-191.
10. Zhang J, Huang X, Wang H, Liu X, Zhang T, et al. (2015) The challenges and promises of allogeneic mesenchymal stem cells for use as a cell-based therapy. Stem Cell Res Ther 6: 234.
11. Ye Y, Zeng YM, Wan MR, Lu XF (2011) Induction of human bone marrow mesenchymal stem cells differentiation into neural-like cells using cerebrospinal fluid. Cell Biochem Biophys 59: 179-184.
12. Han R, Kan Q, Sun Y, Wang S, Zhang G, et al. (2012) MiR-9 promotes the neural differentiation of mouse bone marrow mesenchymal stem cells via targeting zinc finger protein 521. Neurosci Lett 515: 147-152.
13. Sanchez-Ramos J, Song S, Cardozo-Pelaez F, Hazzi C, Stedeford T, et al. (2000) Adult bone marrow stromal cells differentiate into neural cells in vitro. Exp Neurol 164: 247-256.
14. Kabos P, Ehtesham M, Kabosova A, Black KL, Yu JS (2002) Generation of neural progenitor cells from whole adult bone marrow. Exp Neurol 178: 288-293.

15. Tio M, Tan KH, Lee W, Wang TT, Udolph G (2010) Roles of db-cAMP, IBMX and RA in aspects of neural differentiation of cord blood derived mesenchymal-like stem cells. PLoS One 5: e9398.
16. Gustafsson E, Andsberg G, Darsalia V, Mohapel P, Mandel RJ, et al. (2003) Anterograde delivery of brain-derived neurotrophic factor to striatum via nigral transduction of recombinant adeno-associated virus increases neuronal death but promotes neurogenic response following stroke. Eur J Neurosci 17: 2667-2678.
17. Montzka K, Lassonczyk N, Tschoke B, Neuss S, Fuhrmann T, et al. (2009) Neural differentiation potential of human bone marrow-derived mesenchymal stromal cells: misleading marker gene expression. BMC Neurosci 10: 16.
18. Shih CH, Chen CJ, Chen L (2013) New function of the adaptor protein SH2B1 in brain-derived neurotrophic factor-induced neurite outgrowth. PLoS One 8: e79619.
19. Long X, Olszewski M, Huang W, Kletzel M (2005) Neural cell differentiation in vitro from adult human bone marrow mesenchymal stem cells. Stem Cells Dev 14: 65-69.
20. Raedt R, Pinxteren J, Van Dycke A, Waeytens A, Craeye D, et al. (2007) Differentiation assays of bone marrow-derived Multipotent Adult Progenitor Cell (MAPC)-like cells towards neural cells cannot depend on morphology and a limited set of neural markers. Exp Neurol 203: 542-554.
21. Shall G, Menosky M, Decker S, Nethala P, Welchko R, et al. (2018) Effects of Passage Number and Differentiation Protocol on the Generation of Dopaminergic Neurons from Rat Bone Marrow-Derived Mesenchymal Stem Cells. Int J Mol Sci 19.
22. Grade S, Gotz M (2017) Neuronal replacement therapy: previous achievements and challenges ahead. NPJ Regen Med 2: 29.
23. Irion S, Zabierowski SE, Tomishima MJ (2017) Bringing Neural Cell Therapies to the Clinic: Past and Future Strategies. Mol Ther Methods Clin Dev 4: 72-82.
24. Scuteri A, Miloso M, Foudah D, Orciani M, Cavaletti G, et al. (2011) Mesenchymal stem cells neuronal differentiation ability: a real perspective for nervous system repair? Curr Stem Cell Res Ther 6: 82-92.
25. Gordon D, Scolding NJ (2009) Human mesenchymal stem cell culture for neural transplantation. Methods Mol Biol 549: 103-118.
26. Caldwell MA, He X, Wilkie N, Pollack S, Marshall G, et al. (2001) Growth factors regulate the survival and fate of cells derived from human neurospheres. Nat Biotechnol 19: 475-479.
27. Johansson PA, Cappello S, Gotz M (2010) Stem cells niches during development--lessons from the cerebral cortex. Curr Opin Neurobiol 20: 400-407.
28. Moreno Davila H (1999) Molecular and functional diversity of voltage-gated calcium channels. Ann N Y Acad Sci 868: 102-117.
29. Imaizumi K, Ruthazer ES, MacLean JN, Lee CC (2018) Editorial: Spontaneous Activity in Sensory Systems. Front Neural Circuits 12: 27.
30. Hermann A, Liebau S, Gastl R, Fickert S, Habisch HJ, et al. (2006) Comparative analysis of neuroectodermal differentiation capacity of human bone marrow stromal cells using various conversion protocols. J Neurosci Res 83: 1502-1514.
31. Ullah I, Subbarao RB, Rho GJ (2015) Human mesenchymal stem cells - current trends and future prospective. Biosci Rep 35.
32. Boulanger-Weill J, Candat V, Jouary A, Romano SA, Perez-Schuster V, et al. (2017) Functional Interactions between Newborn and Mature Neurons Leading to Integration into Established Neuronal Circuits. Curr Biol 27: 1707-1720 e1705.
33. van Ooyen A, van Pelt J (1994) Activity-dependent neurite outgrowth and neural network development. Prog Brain Res 102: 245-259.
34. Paavilainen T, Pelkonen A, Makinen ME, Peltola M, Huhtala H, et al. (2018) Effect of prolonged differentiation on functional maturation of human pluripotent stem cell-derived neuronal cultures. Stem Cell Res 27: 151-161.

35. Singh M, Kakkar A, Sharma R, Kharbanda OP, Monga N, et al. (2017) Synergistic Effect of BDNF and FGF2 in Efficient Generation of Functional Dopaminergic Neurons from human Mesenchymal Stem Cells. Sci Rep 7: 10378.
36. Goparaju SK, Kohda K, Ibata K, Soma A, Nakatake Y, et al. (2017) Rapid differentiation of human pluripotent stem cells into functional neurons by mRNAs encoding transcription factors. Sci Rep 7: 42367.
37. Ouyang K, Zheng H, Qin X, Zhang C, Yang D, et al. (2005) Ca2+ sparks and secretion in dorsal root ganglion neurons. Proc Natl Acad Sci U S A 102: 12259-12264.
38. Luhmann HJ, Sinning A, Yang JW, Reyes-Puerta V, Stuttgen MC, et al. (2016) Spontaneous Neuronal Activity in Developing Neocortical Networks: From Single Cells to Large-Scale Interactions. Front Neural Circuits 10: 40.
39. Belinsky GS, Rich MT, Sirois CL, Short SM, Pedrosa E, et al. (2014) Patch-clamp recordings and calcium imaging followed by single-cell PCR reveal the developmental profile of 13 genes in iPSC-derived human neurons. Stem Cell Res 12: 101-118.
40. Yu JH, Kim M-S, Lee M-Y, Lee JY, Seo JH, et al. (2014) GABAergic neuronal differentiation induced by brain-derived neurotrophic factor in human mesenchymal stem cells. Animal Cells and Systems 18: 17-24.
41. Hayashi T, Wakao S, Kitada M, Ose T, Watabe H, et al. (2013) Autologous mesenchymal stem cell-derived dopaminergic neurons function in parkinsonian macaques. J Clin Invest 123: 272-284.
42. Park J, Lee N, Lee J, Choe EK, Kim MK, et al. (2017) Small molecule-based lineage switch of human adipose-derived stem cells into neural stem cells and functional GABAergic neurons. Sci Rep 7: 10166.
43. Lindsay SL, Barnett SC (2017) Are nestin-positive mesenchymal stromal cells a better source of cells for CNS repair? Neurochem Int 106: 101-107.
44. Wislet-Gendebien S, Hans G, Leprince P, Rigo JM, Moonen G, et al. (2005) Plasticity of cultured mesenchymal stem cells: switch from nestin-positive to excitable neuron-like phenotype. Stem Cells 23: 392-402.
45. Dimarino AM, Caplan AI, Bonfield TL (2013) Mesenchymal stem cells in tissue repair. Front Immunol 4: 201.
46. Khoo ML, Tao H, Meedeniya AC, Mackay-Sim A, Ma DD (2011) Transplantation of neuronal-primed human bone marrow mesenchymal stem cells in hemiparkinsonian rodents. PLoS One 6: e19025.

MULTIMEDIA FILES

Video 1. Real time Calcium imaging of hMd-Neurons from hMSC cell lines

Video 2. Single cell focusing of Ca imaging in hMd-Neurons from bone marrow donor derived hMSCs.

Video 3. Real time Calcium imaging of hMd-Neurons from bone marrow donor derived hMSCs

Video 4. Real time Calcium imaging in uninduced hMSCs.

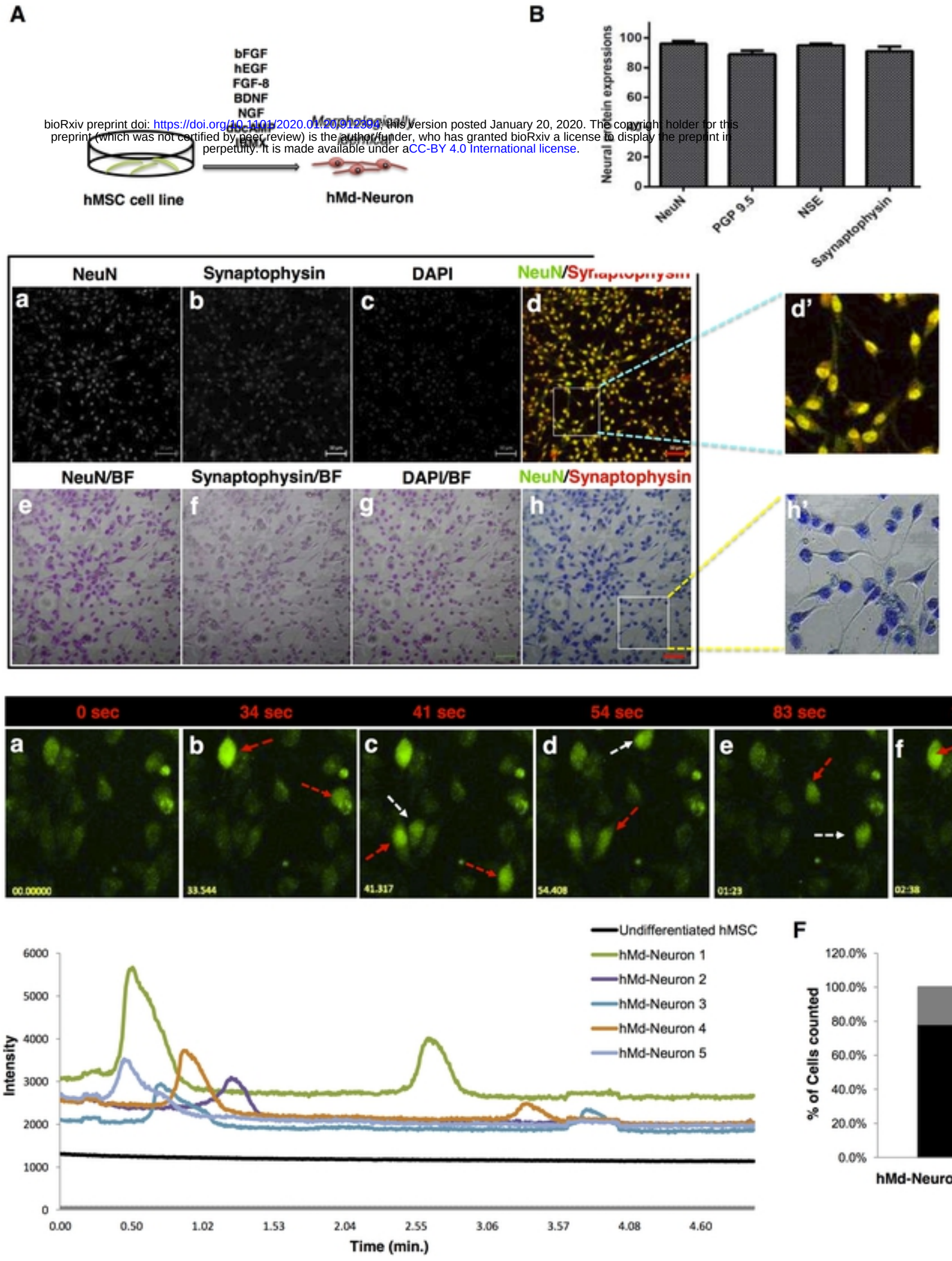

Figure 1

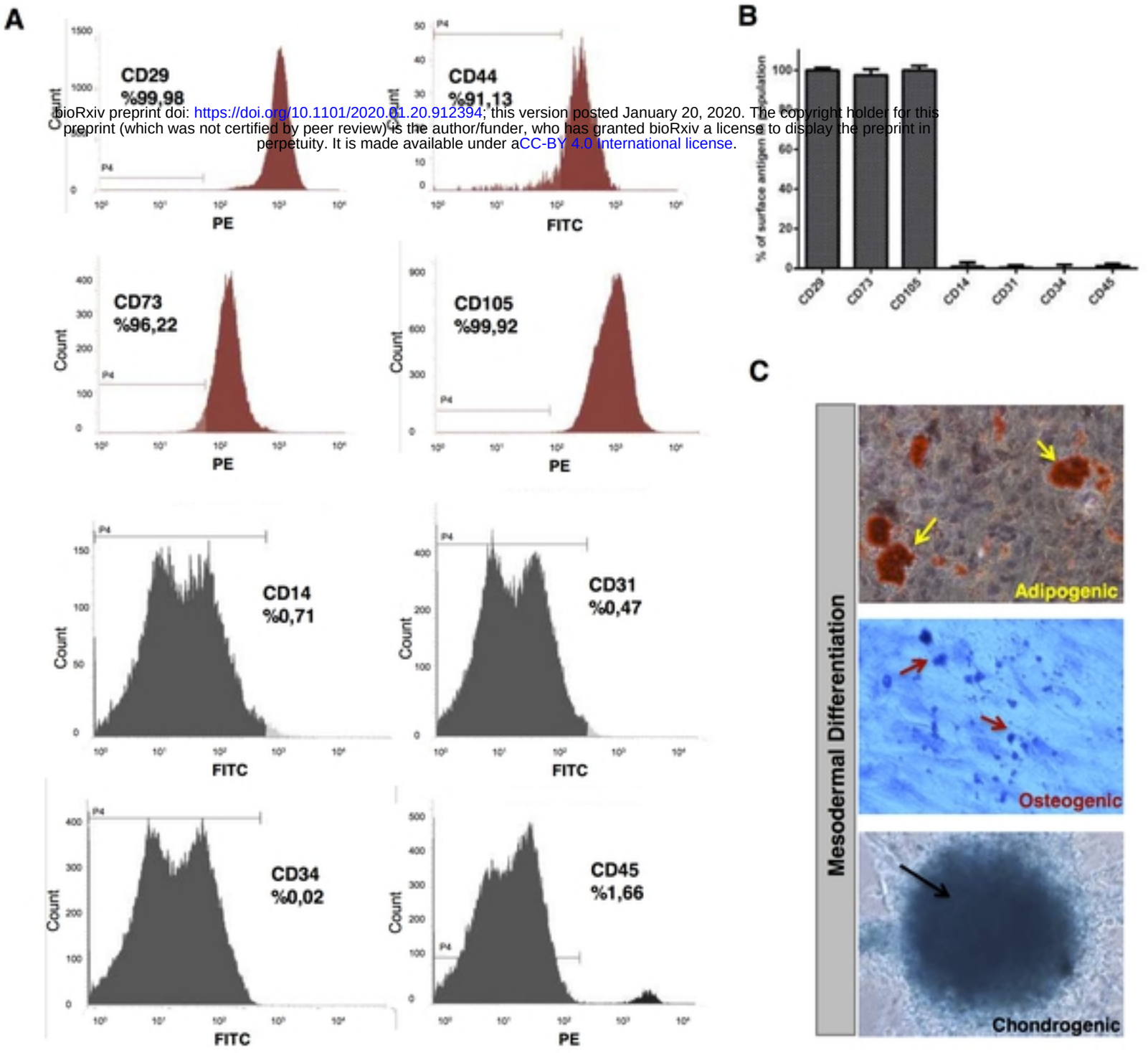

Figure 2

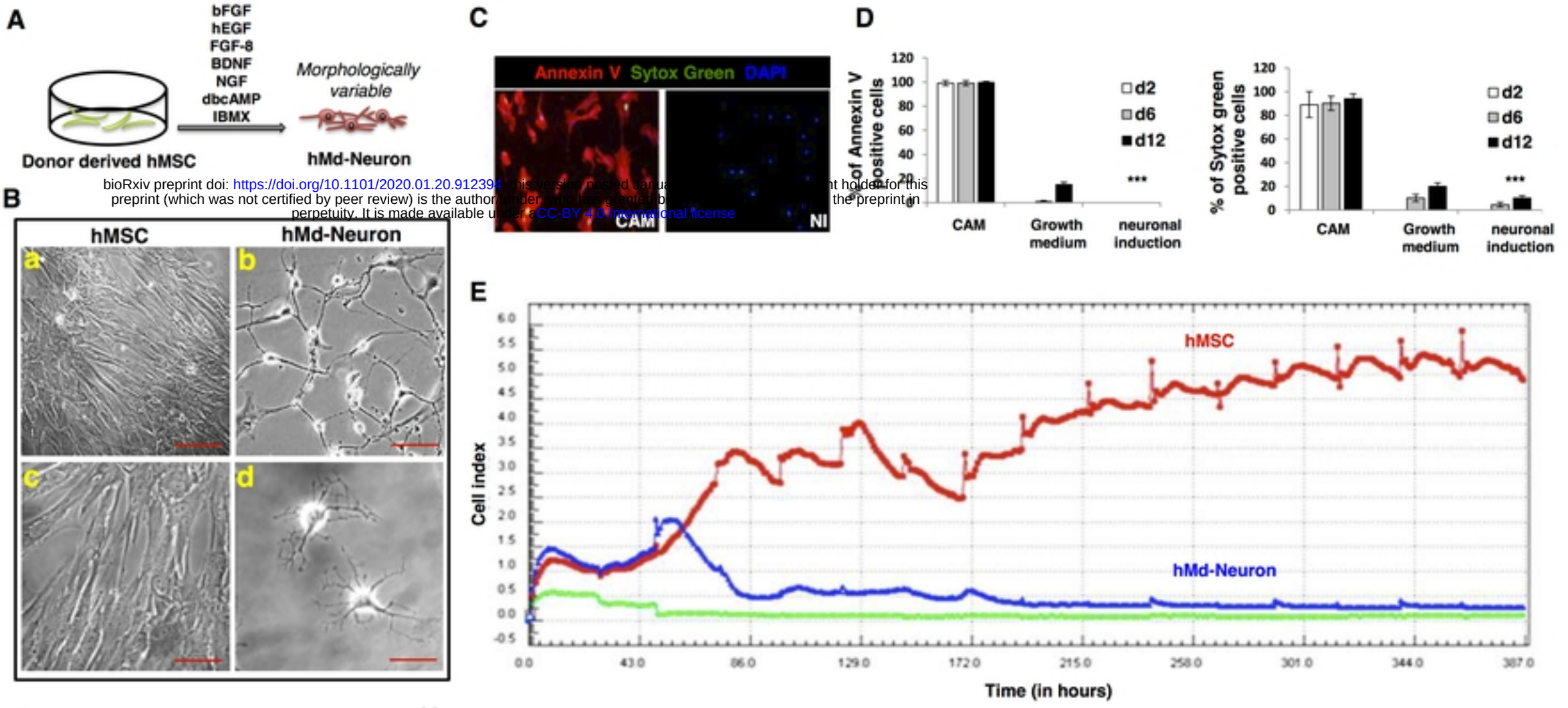

Figure 3

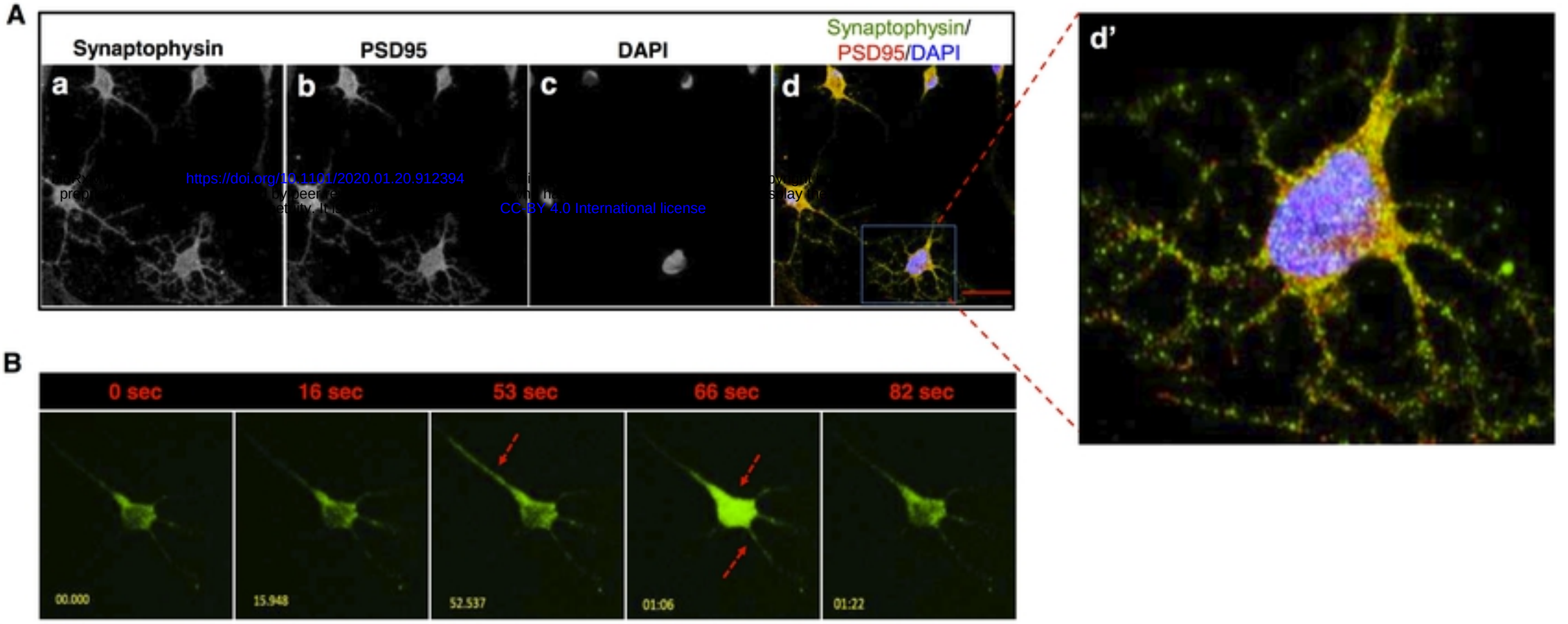

Figure 4